Chip-Type LTCC–MLC Baluns Using the Stepped Impedance Method

Ching-Wen Tang, Jyh-Wen Sheen, and Chi-Yang Chang

***Abstract*—A chip-type low-temperature co-fired ceramic (LTCC) multilayer ceramic (MLC) balun is presented in this paper. This balun is designed using the stepped impedance method. It uses a multilayer structure, meander lines, and multisection coupled lines. The use of multisection couple lines that have various characteristic impedance ratios can shrink the length of a quarter-wavelength coupled-transmission line and makes it very easy to match various impedances of balanced output. The proposed chip-type balun operates over a bandwidth of 2.25–2.65 GHz. The in-band phase and amplitude balances are excellent because of the symmetric structure and transmission-line trimming section. Measured results of the chip-type LTCC–MLC balun match well with the computer simulation.**

***Index Terms*—Balun, chip-type component, LTCC, MLC, multisection coupled lines, stepped impedance method.**

I. Introduction

THE Marchand balun [1] is very popular in the microwave balun and is important in realizing balanced mixers, amplifiers, multipliers, and phase shifters. Various types of balun such as the active balun [2], lumped-type balun [3], toroid-type balun [4], and 180° hybrid balun [5], [6] were proposed. However, due to varying reasons, these baluns cannot meet the requirement for mobile and cellular communications. For the active balun, the transistor can induce the noise and exhaust more energy. With the lumped-type balun, although the use of a lump capacitor and a lump inductor can achieve a compact size, it is difficult to maintain the balanced output characteristics under broader bandwidth. In the case of a toroid-type balun, it is only used below the UHF band. For 180° hybrid balun, it comprises multiple quarter-wave transmission lines that cause a large size.

The multilayer ceramic (MLC) technology seems to be the best solution to realize chip-type elements [7], [8]. However, at the time of this writing, only a few published papers, e.g., [9], describe the laminated balun. Unfortunately, the balun in [9] shows a very narrow bandwidth of the amplitude and phase balance between the two balanced output ports. In addition, the circuit design in [9] requires precise control of the fabricating process.

In this paper, the proposed balun shows a broader bandwidth and allows for looser processing control. Although the balun in [9] shows a wider relative bandwidth of return loss than the proposed balun, the balun in [9] shows a much narrower bandwidth of amplitude and phase balance. Therefore, the proposed balun is much more broad-band, if the balance of amplitude and phase are concerned. The size reduction of the proposed balun is achieved by using of various impedance ratios of multisection coupled line, which can shorten the length of a quarter-wavelength coupled strip-line.

In the case of RF integrated circuit (IC) application, the input/output impedances usually have complex values. For tuning out the imaginary part of the balanced output impedance, a trimming transmission-line section is proposed.

All of the fabricated low-temperature co-fired ceramic–multilayer ceramic (LTCC–MLC) baluns show an excellent match with predicted performance, except for the insertion loss and the amplitude imbalance. The discrepancy is mainly because the simulations are based on the perfect conductor model for every layers of the metal for the sake of time efficiency.

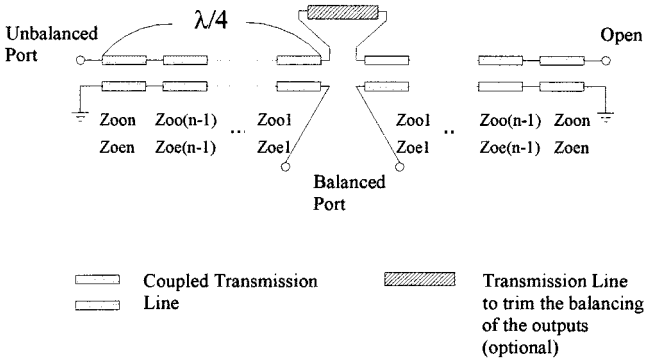

Fig. 1. Equivalent circuit of the LTCC–MLC balun.

II. Theory

Shown in Fig. 1 is the equivalent circuit of the chip type LTCC–MLC balun. This structure is adopted from the concept of the stepped impedance method [10] to shrink the coupled transmission line. It comprises the multisection coupled transmission line and a transmission-line trimming section. Assume that the coupled transmission lines are with the even- and odd-mode impedance of Z_{oei} and Z_{ooi} with respect to section i. Fig. 2 shows the equivalent circuits of the Marchand-type LTCC–MLC balun. Shown in Fig. 2(a) is the simplified coupled-line model of the Marchand balun. At the center frequency, the input impedances of two circuits in Fig. 2(a) are the same as for the balanced port; therefore, the upper circuit in Fig. 2(a) can be equivalent to the lower circuit in Fig. 2(a). Any commercially available circuit simulator can check this. The situation is almost the same in the stepped impedance

Manuscript received March 30, 2001; revised August 2, 2001. This work was supported in part by the Computer and Communication Research Laboratories of the Industrial Technology Research Institute.

C.-W. Tang and C.-Y. Chang are with the Institute of Electrical Communication Engineering, National Chiao Tung University, Hsinchu 300, Taiwan, R.O.C.

J.-W. Sheen is with the Computer and Communication Research Laboratories, Industrial Technology Research Institute, Hsinchu, Taiwan, R.O.C.

Publisher Item Identifier S 0018-9480(01)10459-X.

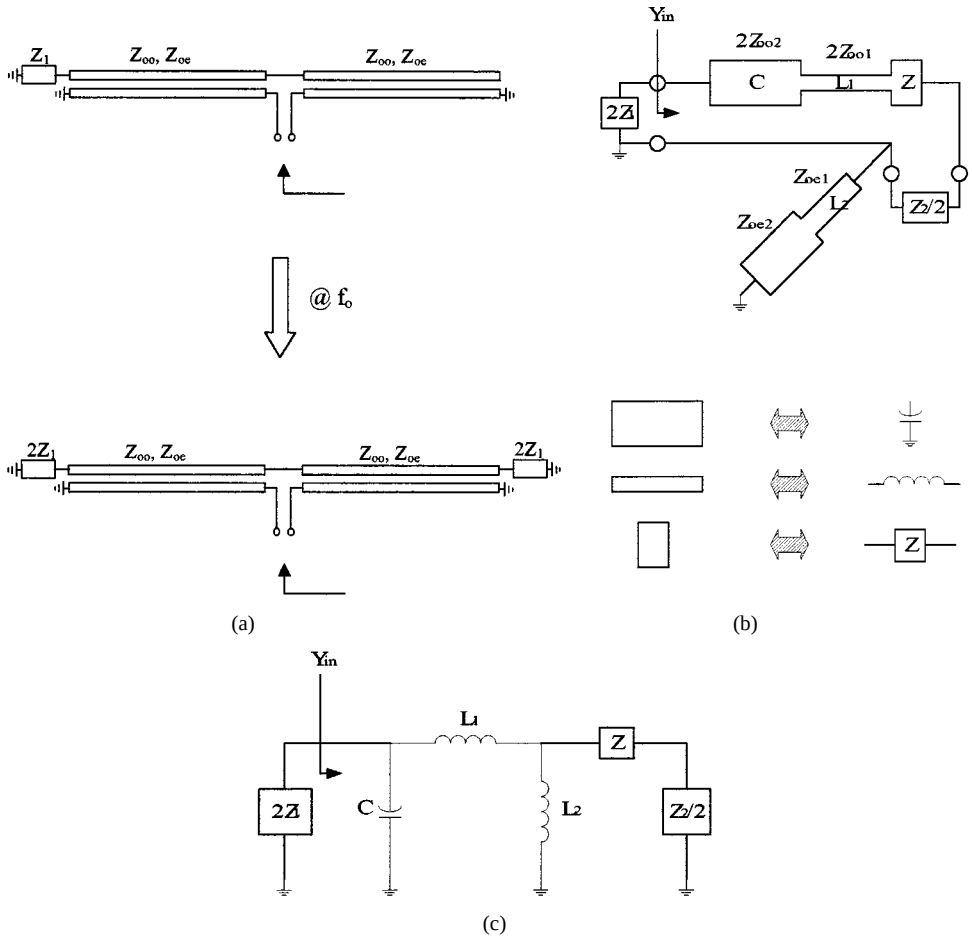

Fig. 2. Principle of impedance translation, which the impedance ratio R is greater than 1/4. (a) The simplified coupled-line model of the Marchand balun. (b) The translation of the left part of Fig. 1 (choosing $n = 2$) and (c) the lumped-element equivalent circuit of Fig. 2(b).

configuration. Choosing $n = 2$ as an example, the circuit can be simplified as shown in Fig. 2(b) [11]. Shown in Fig. 2(c) is the lumped-element equivalent circuit of Fig. 2(b). The equivalence from a transmission line to an inductor or capacitor is also shown at the bottom of Fig. 2(b). This distributed circuit to lumped circuit equivalence is accurate only for a ratio of characteristic impedance of the L-section to that of the C-section to be relatively large. Equation (1) can be obtained from the equivalent circuit of Fig. 2(c) as

$$Y_{\text{in}} \approx \frac{1}{\left(Z+\frac{Z_2}{2}\right)} \cdot \frac{1}{\left(1+\frac{L_1}{L_2}\right)^2 + \left(\frac{\omega L_1}{Z+\frac{Z_2}{2}}\right)^2} + j\left(\omega C - \frac{(L_1+L_2)+\omega^2\left(\frac{1}{Z+\frac{Z_2}{2}}\right)^2 L_1L_2^2}{\omega(L_1+L_2)^2+\omega^3\left(\frac{1}{Z+\frac{Z_2}{2}}\right)^2 L_1^2L_2^2}\right) \quad (1)$$

where Z_2 is the balanced output impedance, which equals $R_2 + jX_2$, Z is the impedance of the transmission-line trimming section, L_1 is the equivalent inductance of a high-impedance coupled line in the unbalance input port, C is the equivalent capacitance of a low-impedance coupled line in the unbalance input port, and L_2 is the equivalent inductance of a high- impedance coupled line in the balance output port.

In most practical applications, the unbalanced input impedance $Z_1(Z_{\text{in}} = 2Z_1$, and $Z_1 = R_1 + jX_1)$ is always 50 Ω. When the impedance of the transmission-line trimming section compensates for the imaginary part of the output impedance, (1) can be abbreviated to

$$Y_{\text{in}} \approx \frac{2}{R_2} \cdot \frac{1}{\left(1+\frac{L_1}{L_2}\right)^2 + \left(\frac{2\omega L_1}{R_2}\right)^2} + j\left(\omega C - \frac{(L_1+L_2)+\omega^2\left(\frac{2}{R_2}\right)^2 L_1L_2^2}{\omega(L_1+L_2)^2+\omega^3\left(\frac{2}{R_2}\right)^2 L_1^2L_2^2}\right) = \frac{2}{R_2} \cdot M(\omega) + jB_1(\omega) \quad (2)$$

where R_2 is the real part of the balanced output impedance, L_1 is the equivalent inductance of a high-impedance coupled line in the unbalance input port, C is the equivalent capacitance of a low-impedance coupled line in the unbalance input port, and L_2 is the equivalent inductance of a narrow coupled line in the balance output port.

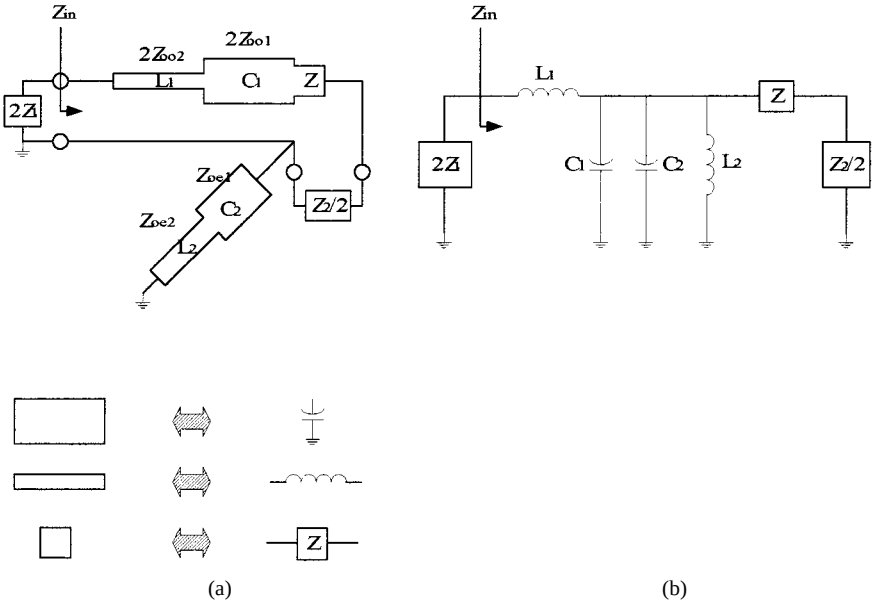

Fig. 3. Principle of impedance translation, for which the impedance ratio R is smaller than 1/4. (a) The translation of the left part of Fig. 1 (choosing $n = 2$) and (b) the lumped-element equivalent circuit of Fig. 3(a).

If the imaginary part $B_1(\omega)$ has been tuned out, the real part of Z_{in} equals $R_2/(2 \cdot M(\omega))$. Because $M(\omega)$ is always smaller than 1, which implies that the ratio R of the unbalanced input impedance to the balanced output impedance $(R = Z_1/Z_2)$ is greater than 1/4. In other words, if Z_1 equals 50 Ω, Z_2 must be smaller than 200 Ω. Properly choosing the values of C and L_1, the imaginary part $B_1(\omega)$ can equal 0. This means that the contribution of L_2 could be canceled. On the other hand, if the value of capacitance C and inductance L_1 is fixed, the transmission line can be shortened with a lower characteristic impedance for the C-section and with higher characteristic impedance for the L_1-section, respectively. This phenomenon of length shrinkage is similar to that of the stepped-impedance resonator [12].

For the case of impedance ratio $R < 1/4$, the position of C and L_1 in Fig. 2(c) must be exchanged; therefore, the high- and low-impedance coupled transmission lines in Fig. 2(b) also need to be exchanged accordingly. The equivalent circuit of the balun should be changed to Fig. 3. According to Fig. 3, the input impedance Z_{in} can be obtained from (3), as shown at the bottom of this page, where Z_2 is the balanced output impedance, which equals $R_2 + jX_2$, Z is the impedance of the transmission line trimming section, L_1 is the equivalent inductance of the high-impedance coupled line in the unbalance input port,

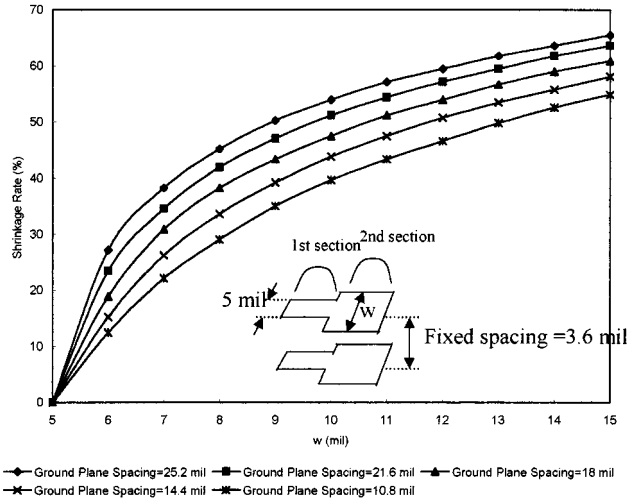

Fig. 4. Shrinkage rate of two-section coupled lines versus different linewidths of the second coupled-line section. (The linewidth of the first coupled line is 5 mil.)

C_1 is the equivalent capacitance of the low-impedance coupled line in the unbalance input port, L_2 is the equivalent inductance of the high-impedance coupled line in the balance output port,

$$Z_{\text{in}} \approx \left(Z + \frac{Z_2}{2}\right) \cdot \frac{1}{1 + \left[\dfrac{Z + \dfrac{Z_2}{2}}{\omega L_2} - \omega(C_1 + C_2)\left(Z + \dfrac{Z_2}{2}\right)\right]^2} + j\left\{\omega L_1 + \frac{\omega L_2\left(Z + \dfrac{Z_2}{2}\right)^2 - \omega^3 L_2^2 (C_1 + C_2)\left(Z + \dfrac{Z_2}{2}\right)^2}{\left[\left(Z + \dfrac{Z_2}{2}\right) - \omega^2 L_2 (C_1 + C_2)\left(Z + \dfrac{Z_2}{2}\right)\right]^2 + (\omega L_2)^2}\right\} \quad (3)$$

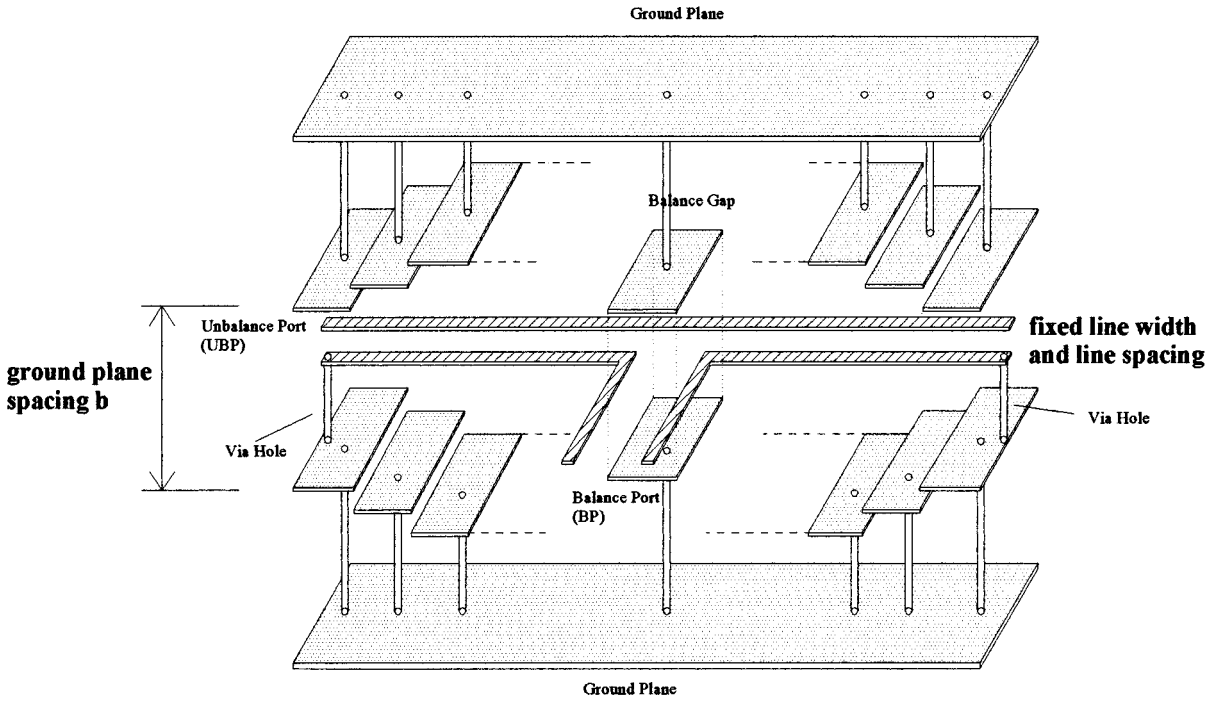

(a)

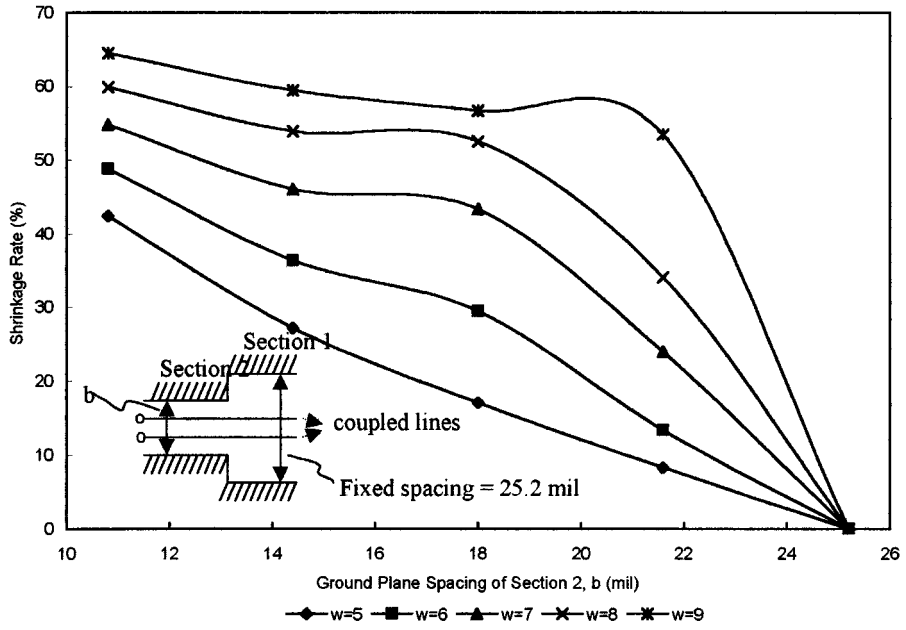

(b)

Fig. 5. Miniaturizing method of using different ground plane spacing for each coupled-line section. (a) The 3-D view of a multisection coupled transmission line using the different layer thickness method. (b) The shrinkage rate of two-section coupled lines versus different ground plane spacing of the second coupled-line section. (Ground plane spacing of section 1 is fixed to be 25.2 mil and the coupled-line spacing is also fixed to be 3.6 mil.)

and C_2 is the equivalent capacitance of the low-impedance coupled line in the balance output port.

If the transmission-line trimming section eliminates the imaginary part of the balanced output impedance, (3) could be simplified to (4), shown at the bottom of the following page.

The impedance ratio $R(R = Z_1/Z_2)$ is smaller than 1/4 because the value of $N(\omega)$ in (4) is smaller than one. In other words, if Z_1 equals 50 Ω, Z_2 must be greater than 200 Ω. The same as for the $R > 1/4$ case, the imaginary part $X_1(\omega)$ of the input impedance can be zero, if the values of L_1, C_1, L_2, and C_2 are properly chosen. According to the theory of stepped impedance resonator, the length of this $R < 1/4$ case should be longer than that of the uniform coupled line.

According to the above analysis, the stepped impedance method is very useful for achieving the impedance transformation. Besides, in the cases of an impedance ratio greater than 1/4 (this is true for most of practical applications), the length of the two coupled-line sections can be shortened.

Equations (1)–(4) are accurate for cases of relatively large ratios of characteristic impedance of the L-section to the C-section. When the characteristic impedance ratio of the two stepped impedance sections as shown in Figs. 2(b) or 3(a) is larger than 1.5 or smaller than 0.5, the values from these equations are sufficiently accurate. After we obtain the values of L and C, the lumped circuit models of Figs. 2(c) and 3(b) are then changed to a distributed circuit model to perform further simulations. For the characteristic impedance ratio between 0.5 and 1.5, the values obtained from these equations need to be modified. The modification can be done using a transmission-line model in a conventional circuit simulator. Finally, the electromagnetic (EM) simulator does the final design to get the precise physical dimensions of the balun.

III. Different Methods to Implement the Stepped Impedance Coupled Lines

We use the two-section stepped impedance method to shrink the size of the MLC-LTCC balun as discussed in previous section. Two methods can realize the proposed two-section stepped impedance coupled lines. The first one uses a broadside coupled line with various linewidth sections. Fig. 4 shows the shrinkage rate of two-section coupled lines versus different linewidth of the second coupled-line section. The corresponding spaces between two ground planes of two-section coupled lines are 25.2, 21.6, 18, 14.4, and 10.8 mil, respectively. In this example, the broadside coupled-line spacing is fixed to be 3.6 mil. When the linewidth of the second coupled-line section is wider, the shrinkage rate is increased as shown in Fig. 4. The second miniaturizing method uses different ground plane spacing for each coupled-line section, as shown in Fig. 5(a). It also has the characteristics of the thinner the ground plane spacing, the higher the shrinkage rate, as shown in Fig. 5(b).

IV. Design Example for 50-Ω Balanced Output Impedance

Theoretically, the proposed balun can have any balanced output impedance. Here, we choose a balun with 50-Ω balanced output impedance at each output port as an example. The chip-type balun is designed to operate in the frequency range of 2.25–2.65 GHz. Unbalanced input impedance is also 50 Ω. The design procedures are as follows. Firstly, we use the circuit simulator such as Libra or equivalent software to obtain the initial design. Secondly, we use the full-wave EM simulator—Sonnet [13] to fine-tune the final physical parameters. Because the structure of the proposed balun is symmetric, it can be separated into two parts and can be folded into upper (or lower) layers. Finally, two coupled center strips can be meandered to shrink the balun further. The structure of LTCC–MLC balun is shown in Fig. 6, which is combined with both shrinkage methods mentioned in the previous section.

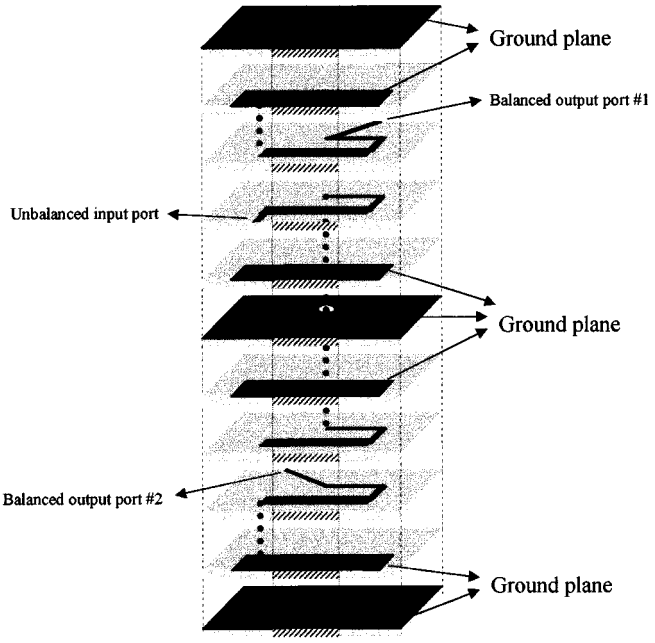

Fig. 6. Proposed multilayer structure of the LTCC–MLC balun. (The slanted lines represent the vertical connection between different metal layers.)

The simulated results are shown in Fig. 7. The insertion loss and the return loss are less than -0.32 dB and -16.5 dB, respectively, in the operating frequency range as shown in Fig. 7(a). The amplitude and phase imbalance between the balanced outputs are within 0.47 dB and 0.85°, respectively, over the operating frequency range as shown in Fig. 7(b).

Fig. 8 shows the photograph of a fabricated LTCC–MLC balun. The designed chip-type balun is fabricated with a multilayer configuration using 90-μm-thick ceramic sheets $(\varepsilon r = 7.8)$ and a 10-μm-thick Ag metal pattern. The overall size of the balun is 3.2 mm × 1.6 mm × 1.0 mm. The measured results are shown in Fig. 9. The insertion loss and return loss are less than -1.02 and -14.5 dB, respectively, over the operating frequency band as shown in Fig. 9(a). Fig. 9(b) shows the measured amplitude and phase difference between balanced outputs. The amplitude and phase imbalances are within 0.43 dB and 1.23°, respectively, over the operating frequency range. Comparing Figs. 7 and 9, the excellent match between the theoretical and measured results is obtained except for the insertion loss. The measured insertion loss is higher than the simulated result because the substrate loss and the

$$Z_{\text{in}} \approx \frac{R_2}{2} \cdot \frac{1}{1+\left[\dfrac{R_2}{2\omega L_2} - \omega(C_1+C_2)\dfrac{R_2}{2}\right]^2} + j\left\{\omega L_1 + \frac{\omega L_2\left(\dfrac{R_2}{2}\right)^2 - \omega^3 L_2^2(C_1+C_2)\left(\dfrac{R_2}{2}\right)^2}{\left[\dfrac{R_2}{2} - \omega^2 L_2(C_1+C_2)\left(\dfrac{R_2}{2}\right)\right]^2 + (\omega L_2)^2}\right\}$$
$$= \frac{R_2}{2} \cdot N(\omega) + jX_1(\omega) \tag{4}$$

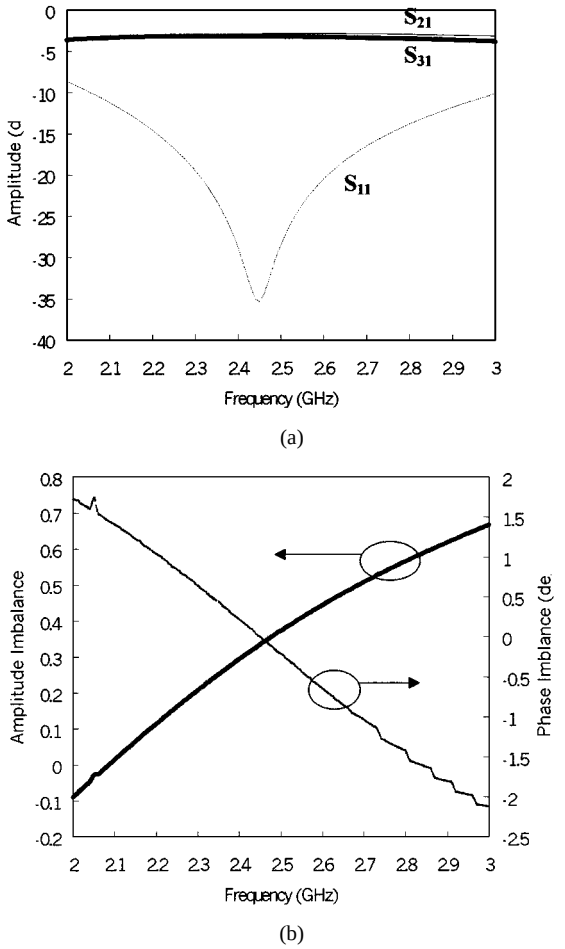

Fig. 7. Smulated results of designed chip-type balun. (a) The insertion loss and return loss. (b) The amplitude and phase imbalance between the balanced outputs.

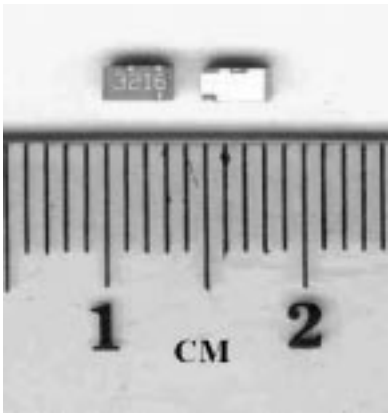

Fig. 8. Photograph of the fabricated chip-type balun.

metal loss are not included in the simulation for simulation speed consideration.

V. Transmission-Line Trimming Section for Matching With the Complex Load

Recently, short-range wireless communication such as bluetooth becomes more and more important. The RF ICs such as those for bluetooth applications are usually used with balanced input/output ports.

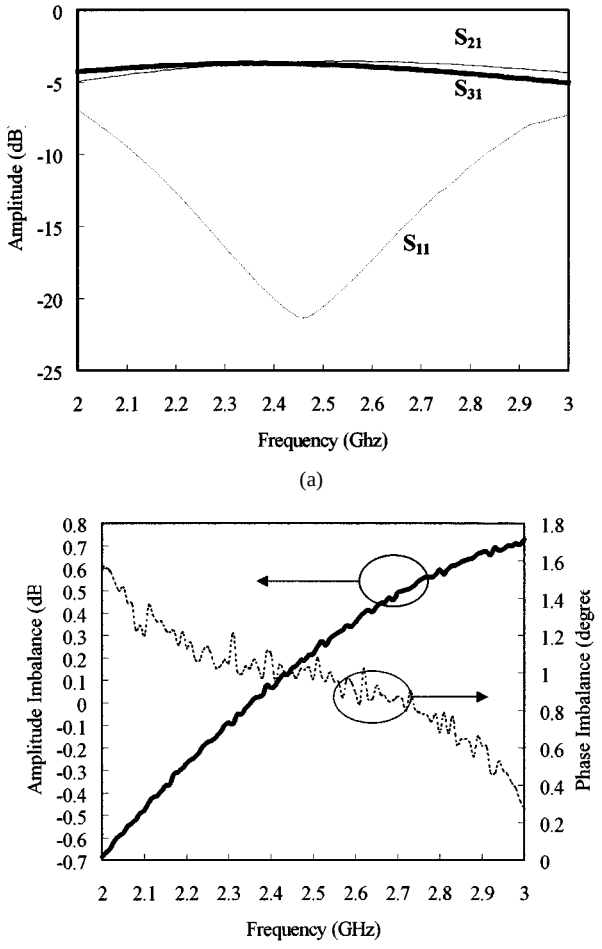

Fig. 9. Measured results of a fabricated chip-type balun. (a) The insertion loss and return loss. (b) The amplitude and phase imbalance between balanced outputs.

In the design of a bluetooth module, the balun must realize the impedance transformation and connect other unbalanced RF circuits. The conventional design of a balun has the characteristic of real-valued output impedance, but the input/output impedance of a differential RF IC are mostly complex values. Using the proposed transmission-line trimming section in our balun design as shown in Fig. 1 can achieve the cancellation of the imaginary part of the complex load impedance.

Here, we show design examples that two bluetooth RF ICs, namely a low-noise amplifier and a driver amplifier, connect with two proposed LTCC–MLC baluns. To show the effect of the transmission-line trimming section, each of the LTCC–MLC baluns has two versions: the first version is the balun without the transmission-line trimming section, and the second version is with the transmission-line trimming section. Fig. 10 shows the comparison of the performances that does and does not include the transmission-line trimming section in connection with the bluetooth RF ICs. The test setup is combined with a bluetooth amplifier as shown in Fig. 10(a), because the amplifier impedance is a complex value and not suitable for measuring in a 50-Ω testing system. Shown in Fig. 10(b) is a balun with a bluetooth low-noise amplifier, and shown in Fig. 10(c) is a balun with a bluetooth driver amplifier.

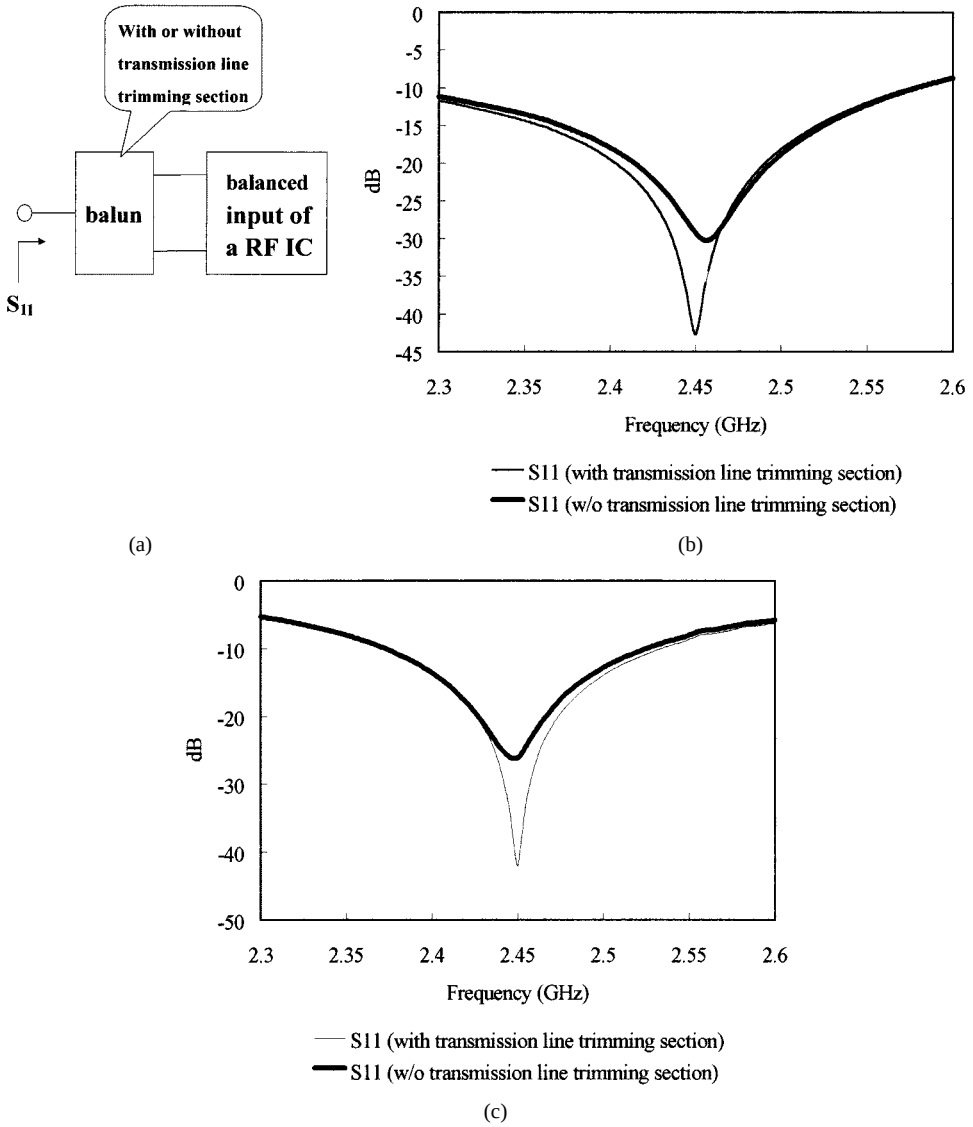

Fig. 10. Comparison of the performances that do and do not include the transmission-line trimming section in connection with bluetooth RF ICs. (a) The test setup is combined with the LTCC–MLC balun and the bluetooth amplifier. (b) The balun is combined with the bluetooth low-noise amplifier. (c) The balun is combined with the bluetooth driver amplifier.

The baluns using the proposed transmission-line trimming section achieves better matching performance in both cases.

VI. Conclusion

The novel LTCC–MLC balun has been developed. The equivalent circuit and the design equations of this balun have been given. The design procedures were simple, the size of this balun was compact, and the measured performances matched with simulated results very well. The baluns have been designed for use in the 2.4-GHz ISM frequency band. In the first example, the unbalanced input impedance and the balanced output impedance were both 50 Ω. The measured insertion loss and return loss were less than −1.02 and −14.5 dB, respectively, over the operating frequency band. The measured amplitude and phase imbalances between balanced outputs were within 0.43 dB and 1.23°, respectively, over the operating frequency range. The simulated and measured results showed the validity of the proposed design method. In the second example, a proposed transmission-line trimming section in the balun was useful to achieve a better matching performance of a balanced output port with complex impedance. All of the proposed baluns were fabricated with a multilayered configuration.

Acknowledgment

The authors would like to thank the staff of the Material Research Laboratories, Industrial Technology Research Institute, Hsinchu, Taiwan, R.O.C., for the manufacturing of the MLC balun and the improving of the LTCC processes. The authors also wish thank Dr. W.-J. Tseng and the reviewers of this paper for their helpful comments.

References

[1] N. Marchand, "Transmission line conversion transformers," *Electronics*, vol. 17, no. 12, pp. 142–145, Dec. 1942.
[2] W. S. Titus and M. J. Schindler, "Active balun," U.S. Patent 4 994 755, Feb. 19, 1991.

[3] T. R. Apel and C. E. Page, "Lumped parameter balun," U.S. Patent 5 574 411, Nov. 12, 1996.
[4] M. Onizuka and K. Sato, "BALUN transformer core material, BALUN transformer core and BALUN transformer," U.S. Patent 6 033 593, Mar. 7, 2000.
[5] S. A. Maas, *Microwave Mixers*, 2nd ed. Norwood, MA: Artech House, 1993, pp. 244–247.
[6] J. M. Garcia, "Compact low-loss microwave balun," U.S. Patent 5 455 545, Oct. 3, 1995.
[7] T. Ishizaki and T. Uwano, "A stepped impedance comb-line filter fabricated by using ceramic lamination technique," in *IEEE MTT-S Int. Microwave Symp. Dig.*, 1994, pp. 617–620.
[8] T. Ishizaki, H. Miyake, T. Yamada, H. Kagata, H. Kushitani, and K. Ogawa, "A first practical model of very small and low insertion laminated duplexer using LTCC suitable for W-CDMA portable telephones," in *IEEE MTT-S Int. Microwave Symp. Dig.*, 2000, pp. 187–190.
[9] D. W. Lew, J. S. Park, D. Ahn, N. K. Kang, I. S. Park, W. Lim, and C. S. Too, "A design of the ceramic multiplayer chip balun," in *IEEE MTT-S Int. Microwave Symp. Dig.*, 1999, pp. 1893–1896.
[10] J. W. Sheen, "Miniaturized balun transformer," U.S. Patent 6 133 806, Oct. 17, 2000.
[11] A. Riddle, "Ferrite and wire baluns with under 1dB loss to 2.5 GHz," in *IEEE MTT-S Int. Microwave Symp. Dig.*, 1998, pp. 617–620.
[12] M. Makimoto and S. Yamashita, "Compact bandpass filter using stepped impedance resonators," *Proc. IEEE*, vol. 67, pp. 16–19, Jan. 1979.
[13] *em User's Manual Version 6.0*, Sonnet Software Inc., Liverpool, NY, 1999.

Ching-Wen Tang, photograph and biography not available at the time of publication.

Jyh-Wen Sheen, photograph and biography not available at the time of publication.

Chi-Yang Chang, photograph and biography not available at the time of publication.